

Article

Modulation of the Selectivity in Anions Recognition Processes by Combining Hydrogen- and Halogen-Bonding Interactions

Fabiola Zapata, Sergio J. Benítez-Benítez, Paula Sabater, Antonio Caballero * 
and Pedro Molina * 

Dpto de Química Orgánica, Universidad de Murcia, Campus de Espinardo, E-30100 Murcia, Spain; fazafer@um.es (F.Z.); sergiojose.benitez@um.es (S.J.B.-B.); paula.sabater@um.es (P.S.)

* Correspondence: antocaba@um.es (A.C.); pmolina@um.es (P.M.)

Received: 17 November 2017; Accepted: 18 December 2017; Published: 20 December 2017

Abstract: Most of the halogen bonding receptors for anions described use halogen bonding binding sites solely in the anion recognition process; only a few examples report the study of anion receptors in which the halogen bonding interaction has been used in combination with any other non-covalent interaction. With the aims to extend the knowledge in the behaviour of this kind of mixed receptors, we report here the synthesis and the anion recognition and sensing properties of a new halogen- and hydrogen- bonding receptor which binds anions by the cooperation of both non-covalent interactions. Fluorescence studies showed that the behaviour observed in the anion recognition sensing is similar to the one previously described for the halogen analogue and is quite different to the hydrogen one. On the other hand, the association constants obtained by $^1\text{H-NMR}$ data demonstrate that the mixed halogen- and hydrogen-bonding receptor is more selective for SO_4^{2-} anion than the halogen or hydrogen analogues.

Keywords: halogen-bonding; hydrogen-bonding; anion; fluorescence; imidazolium; recognition; sensing

1. Introduction

The field of anion recognition chemistry has become one of the most important areas in supramolecular chemistry due to the important role that anions play in numerous biological and environmental processes [1–4].

The hydrogen bond (HB) has been probably the most non-covalent interaction used in the design of anion receptors in the last two decades in which amides [5], ureas [6], pyrroles [7] or imidazole [8,9] among others have been used as hydrogen donors as anion binding sites.

The use of the halogen bonding (XB) interaction as an alternative to the hydrogen bonding in the design of new anion receptors has emerged strongly in the last years. Halogen bonding is a noncovalent bonding interaction between halogen atoms that function as electrophilic centers (Lewis acids) and neutral or anionic Lewis bases [10]. Theoretical calculations indicate that the origin of this attraction arises from the positive electrostatic potential located at the terminus of the R–X axis (σ hole), thus resulting in a strongly linear geometry that maximizes the interface of opposite charges [11]. Although a number of solid state examples and theoretical studies revealed the potential of halogen bonding interactions for anion recognition, only very recently has it been exploited in solution phase. Practically all the halogen bonding receptors for anion described in the literature use halogen bonding binding sites solely to bind anions. Despite that the combination of two or more different non-covalent interactions in the same receptors is becoming an emerging strategy in the design of new anion receptors [12], only a few examples use the halogen bonding interaction in combination with others in the anion recognition process [13–23].

Recently, we have reported the synthesis and the anion sensing properties of two-armed charge-assisted ditopic imidazolium and haloimidazolium bidentate receptors which recognize anions by hydrogen or halogen bonding interaction, respectively [24]. Taking into account the important differences found in the sensing behavior between these two receptors, we decided to perform the synthesis and study of a new charge-assisted bidentate receptor containing both halogen and hydrogen bonding sites by incorporation in its structure of one haloimidazolium, halogen bonding binding site, and one imidazolium, hydrogen bonding binding site, which could act through the cooperative and simultaneous action of halogen bonds and hydrogen bonds during the anion recognition event. The receptor also incorporates two end-capped photoactive anthracene rings as fluorescent signaling units into this host framework (Figure 1).

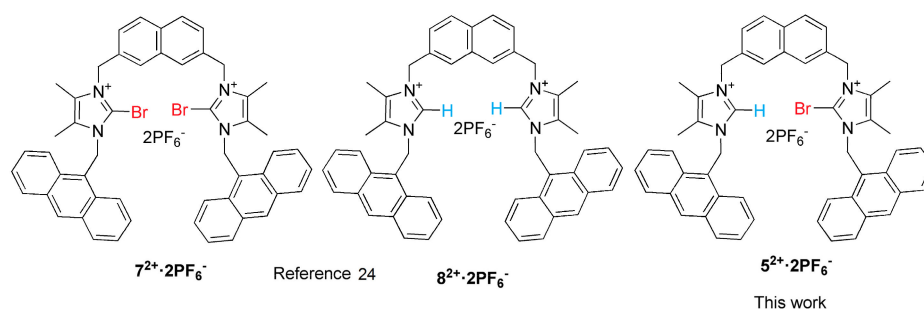


Figure 1. Structure of the halogen and hydrogen bonding receptors $7^{2+} \cdot 2PF_6^{-}$ and $8^{2+} \cdot 2PF_6^{-}$ reported in [24] and the structure of the mixed halogen and hydrogen bonding receptor $5^{2+} \cdot 2PF_6^{-}$ proposed in this work.

2. Results and Discussion

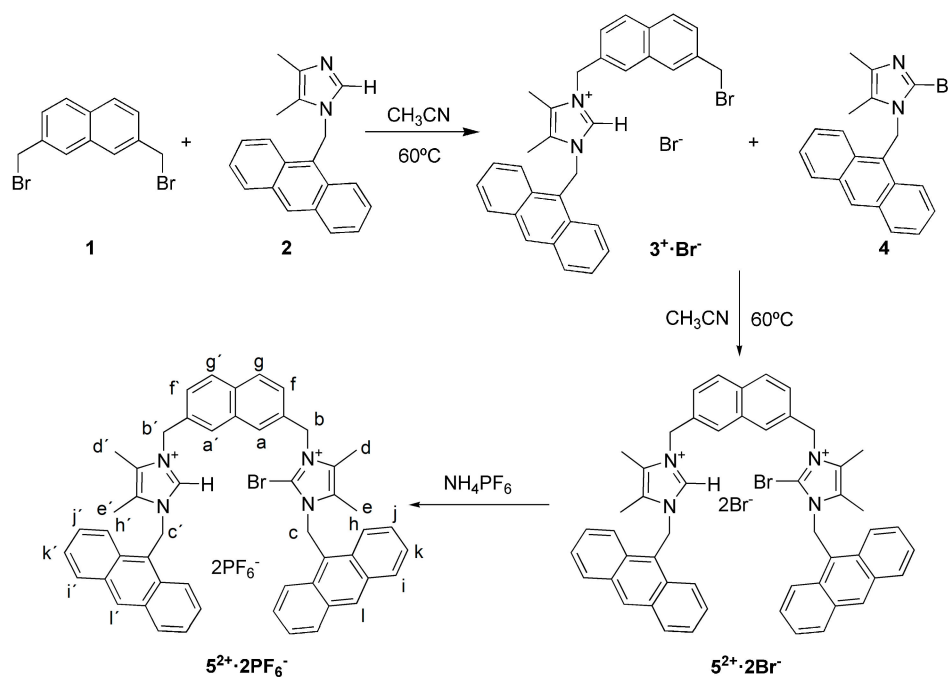
2.1. Synthesis

The novel bis-imidazolium receptor $5^{2+} \cdot 2PF_6^{-}$ was prepared with a 31% overall yield by a stepwise procedure that involved the alkylation of 1-((anthracen-9-yl)methyl)-4,5-dimethyl-1H-imidazole **2** with 2,7-bis(bromomethyl)naphthalene **1**, providing the intermediate $3^{+} \cdot Br^{-}$ (63% yield), which was reacted with 1-((anthracen-9-yl)methyl)-2-bromo-4,5-dimethyl-1H-imidazole **4**, yielding the receptor as bromide salt in moderate yield (25%). Anion exchange with the corresponding hexafluorophosphate salt was achieved on addition of aqueous NH_4PF_6 . The compounds **2** and **4** were synthesized by alkylation of 4,5-dimethyl-1H-imidazole [25] and 2-bromo-4,5-dimethyl-1H-imidazole [26] with 9-(bromomethyl)anthracene, respectively (Scheme 1).

2.2. Anion Binding Studies

The binding and sensing ability of the receptor $5^{2+} \cdot 2PF_6^{-}$ toward several anions (F^{-} , Cl^{-} , Br^{-} , I^{-} , SO_4^{2-} , HSO_4^{-} , $PhCOO^{-}$, ClO_4^{-} , $HP_2O_7^{3-}$, AcO^{-} , NO_3^{-} and $H_2PO_4^{-}$) as tetrabutylammonium salts were investigated by spectroscopic measurements and 1H -NMR spectroscopy.

The emission spectrum of the receptor $5^{2+} \cdot 2PF_6^{-}$ ($\Phi = 0.036$) in CH_3CN showed the characteristic anthracene monomeric bands at $\lambda = 396, 418$ and 442 nm, when excited at $\lambda = 370$ nm. The addition of the above-mentioned set of anions to a solution of the receptor $5^{2+} \cdot 2PF_6^{-}$ in CH_3CN ($c = 1 \times 10^{-5}$ M) showed that Cl^{-} , Br^{-} , I^{-} , HSO_4^{-} , $PhCOO^{-}$, ClO_4^{-} and NO_3^{-} anions had no effect on the emission spectrum, whereas the addition of F^{-} , $HP_2O_7^{3-}$, SO_4^{2-} , AcO^{-} and $H_2PO_4^{-}$ anions promoted significant changes in the emission spectrum of receptor $5^{2+} \cdot 2PF_6^{-}$. These changes were strongly dependent on the anion added and different responses have been observed (Figure 2).



Scheme 1. Synthesis of the halogen and hydrogen bonding receptor $5^{2+} \cdot 2PF_6^{-}$.

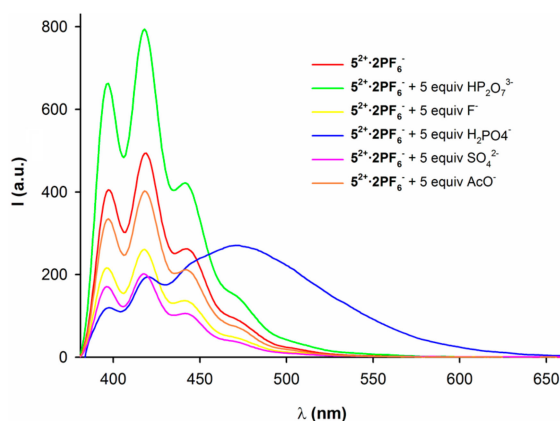


Figure 2. Emission spectrum of the receptor $5^{2+} \cdot 2PF_6^{-}$ ($c = 1 \times 10^{-5}$ M) in CH_3CN (red line) and after the addition of 5 equiv. of $H_2PO_4^{-}$ (blue line), SO_4^{2-} (pink line), AcO^{-} (orange line), $HP_2O_7^{3-}$ (green line) and F^{-} (yellow line).

The presence of AcO^{-} (Figure S3, Supplementary Material) and SO_4^{2-} anions (Figure 3a) induced a decrease in the monomer emission band at $\lambda = 419$ nm of the receptor $5^{2+} \cdot 2PF_6^{-}$ $I_{\text{receptor}}/I_{\text{complex}} = 2.55$ and 2.13, respectively, and also a decrease of the quantum yield from $\Phi = 0.036$ to $\Phi = 0.025$ for AcO^{-} and $\Phi = 0.019$ for SO_4^{2-} anions. A different fluorescent response was observed for $H_2PO_4^{-}$ anions (Figure 3b) in which the presence of this anion promoted a remarkable decrease of the monomer emission bands at $\lambda = 396$, 418 and 412 nm and a progressive increase in a new broad and structureless emission band at $\lambda = 465$ nm, attributed to the anthracene excimer emission band ($\Phi = 0.058$) and finally, when $HP_2O_7^{3-}$ (Figure 3c) and F^{-} (Figures S1 and S2) anions were added, two different effects were observed: first the addition up to 1.8 equiv. of $HP_2O_7^{3-}$ anions or 1 equiv. F^{-} anion induced an increase in the monomer emission band of the receptor, subsequent addition of more than 1.8 equiv. of $HP_2O_7^{3-}$ anions and 1 equiv. in the case of F^{-} , promoted a continuous decrease in the monomer emission band.

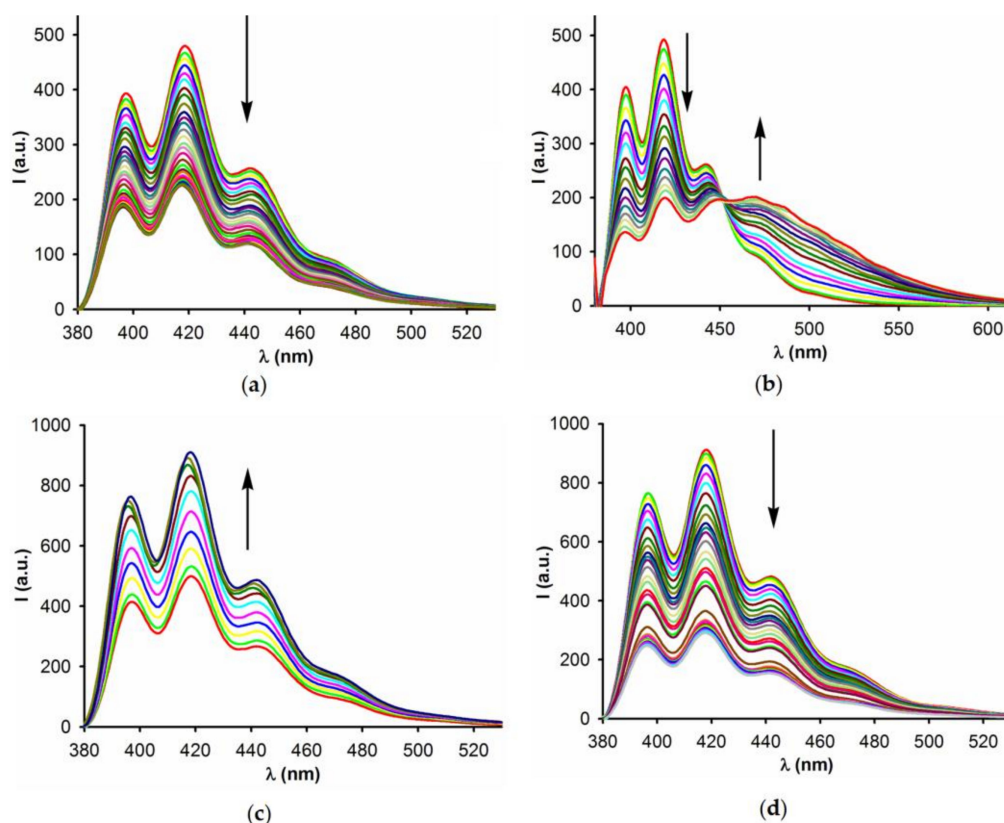


Figure 3. Changes in the fluorescence spectra of receptor $5^{2+} \cdot 2PF_6^{-}$ ($c = 1 \times 10^{-5}$ M) in CH_3CN upon addition of (a) SO_4^{2-} , (b) $H_2PO_4^{-}$, (c) $HP_2O_7^{3-}$ from 0 to 1.8 equiv., and (d) $HP_2O_7^{3-}$ from 1.8 to 100 equiv. Arrows indicate the emission bands that increase or decrease during the titration.

A comparative analysis of the response observed in the fluorescence study indicates that the mixed hydrogen- and halogen- bonding receptor $5^{2+} \cdot 2PF_6^{-}$ shows changes similar to the halogen bonding receptor $7^{2+} \cdot 2PF_6^{-}$. Both receptors $5^{2+} \cdot 2PF_6^{-}$ (HB and XB) and $7^{2+} \cdot 2PF_6^{-}$ (XB) act through a photoinduced electron transfer (PET) mechanism in the presence of SO_4^{2-} anions, and therefore a decrease in the intensity of the emission bands was observed [27]. In addition, a broad emission band at $\lambda = 465$ nm due to a π -stacking interaction between the two anthracene units [28] appears in the spectrum of the receptor $5^{2+} \cdot 2PF_6^{-}$ during the addition of $H_2PO_4^{-}$ anions as it was also observed in the halogen bonding receptor $7^{2+} \cdot 2PF_6^{-}$. Interestingly, the remarkable changes observed in the emission spectrum of the receptor $5^{2+} \cdot 2PF_6^{-}$ after addition of $HP_2O_7^{3-}$ and F^{-} anions are consistent with a chemodosimeter behavior, which was also observed in the halogen bonding receptor $7^{2+} \cdot 2PF_6^{-}$. Interestingly, the emission spectrum of the receptor $5^{2+} \cdot 2PF_6^{-}$ undergoes important changes in the presence of AcO^{-} anions to difference with the described for the halogen bonding receptor $7^{2+} \cdot 2PF_6^{-}$, whereas the behavior towards $H_2PO_4^{-}$ and SO_4^{2-} anions is similar to that found for $7^{2+} \cdot 2PF_6^{-}$. On the other hand, the fluorescent response of the mixed XB and HB receptor $5^{2+} \cdot 2PF_6^{-}$ is quite different than for the hydrogen bonding receptor $8^{2+} \cdot 2PF_6^{-}$, in which the receptor acted on by a photoinduced electron transfer mechanism with all the tested anions.

The stoichiometry of the complexes was determinate by Job-plot experiments using the changes in the fluorogenic response of the receptor $5^{2+} \cdot 2PF_6^{-}$ in the presence of varying concentrations of the tested anions. The results clearly indicated the formation of 1:2 complexes in the case of $H_2PO_4^{-}$ (Figure S7) and AcO^{-} anions (Figure S9), and 1:1 for SO_4^{2-} anions (Figure S8). The association constant values were calculated by fitting the fluorescence data in CH_3CN with the host-guest binding model obtained using the Dynafit program [29] and are summarized in Table 1 together with the values previously reported for the halogen bonding receptor $7^{2+} \cdot 2PF_6^{-}$ and the hydrogen bonding

receptor $8^{2+} \cdot 2PF_6^-$. The association constants obtained indicate that the hydrogen bonding receptor $8^{2+} \cdot 2PF_6^-$ binds the recognized anions stronger than the analogous halogen $7^{2+} \cdot 2PF_6^-$ or the mixed halogen and hydrogen bonding receptor $5^{2+} \cdot 2PF_6^-$ in the pure organic solvent CH_3CN , while the monohalogenated receptor $5^{2+} \cdot 2PF_6^-$ and the dihalogenated receptor $7^{2+} \cdot 2PF_6^-$ bind the anions with similar strength.

Table 1. Association constants for receptor $5^{2+} \cdot PF_6^-$, $7^{2+} \cdot 2PF_6^-$ and $8^{2+} \cdot 2PF_6^-$ with $H_2PO_4^-$, SO_4^{2-} and AcO^- anions in CH_3CN measured by fluorescence technique. Errors (in percent) are given in parentheses.

Receptor	$H_2PO_4^-$	SO_4^{2-}	AcO^-
$5^{2+} \cdot PF_6^-$	$\beta = 5.9 \times 10^{10} M^{-2}$ (15)	$K = 5.7 \times 10^4 M^{-1}$ (14)	$\beta = 2.16 \times 10^9 M^{-2}$ (10)
$7^{2+} \cdot 2PF_6^-$	$\beta = 5.0 \times 10^{11} M^{-2}$ (16)	$K = 8.0 \times 10^4 M^{-1}$ (14)	-
$8^{2+} \cdot 2PF_6^-$	$\beta = 9.8 \times 10^{11} M^{-2}$ (13)	$K = 1.4 \times 10^6 M^{-1}$ (6)	-

The calculated detection limits of the receptor $5^{2+} \cdot 2PF_6^-$ for $H_2PO_4^-$, SO_4^{2-} , and AcO^- anions were $3.90 \times 10^{-6} M$, $3.57 \times 10^{-5} M$, and $4.59 \times 10^{-5} M$ respectively (Figures S4–S6).

The recognition properties of the receptor towards the above-mentioned set of anions were also evaluated by UV-vis spectroscopy. Absorption spectrum of the receptor $5^{2+} \cdot 2PF_6^-$ in CH_3CN ($c = 1 \times 10^{-5} M$) displays two intense absorption bands at $\lambda = 230$ nm ($\epsilon = 1.31 \times 10^5 M^{-1} cm^{-1}$) and $\lambda = 255$ nm ($\epsilon = 2.39 \times 10^5 M^{-1} cm^{-1}$) along with the characteristic absorption bands attributed to the anthracene moieties at $\lambda = 334$ nm ($\epsilon = 6 \times 10^3 M^{-1} cm^{-1}$), $\lambda = 351$ nm ($\epsilon = 11.14 \times 10^4 M^{-1} cm^{-1}$), $\lambda = 370$ nm ($\epsilon = 1.5 \times 10^4 M^{-1} cm^{-1}$) and $\lambda = 390$ nm ($\epsilon = 1.35 \times 10^4 M^{-1} cm^{-1}$). The addition of increase amounts of SO_4^{2-} , AcO^- , $HP_2O_7^{3-}$ and F^- anions to a solution of the receptor in CH_3CN ($c = 1 \times 10^{-5} M$) caused small perturbations in the absorption spectrum of the receptor; by contrast, the addition of $H_2PO_4^-$ anions induced a decrease in the absorption bands at $\lambda = 250$ and $\lambda = 255$ nm while a decrease and red-shifted $\Delta\lambda = 2$ nm in the anthracene absorption bands was observed. The well-defined isosbestic point observed at $\lambda = 260$, $\lambda = 343$, $\lambda = 373$, $\lambda = 382$ and $\lambda = 390$ nm indicates that a neat interconversion between the uncomplexed and complexed species occurs (Figure 4). Unfortunately, these changes do not allow an accurate determination of the association constant.

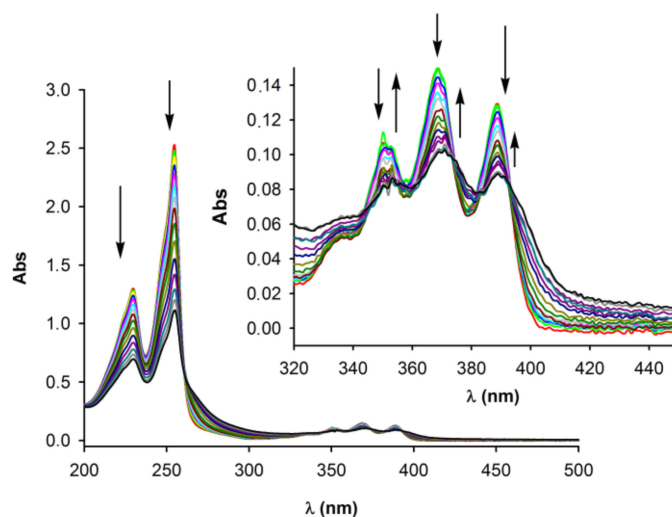


Figure 4. Changes in the absorption spectra of the receptor $5^{2+} \cdot 2PF_6^-$ ($c = 1 \times 10^{-5} M$ in CH_3CN) upon addition of increasing amounts of $H_2PO_4^-$ anions. Arrows indicate the absorption bands that increase or decrease during the titration.

In order to obtain additional information about the binding mode of the receptor $5^{2+} \cdot 2PF_6^-$ with the previously tested anions, 1H -NMR titration experiments were performed. The 1H -NMR

spectrum of the receptor in CD₃CN/CD₃OD (8/2) exhibit the following characteristic signals: (a) the protons of the methyl groups of the Br-imidazolium unit appears at $\delta = 1.86$ and 2.15 ppm and the ones corresponding to the H-imidazolium moiety at $\delta = 2.15$ and 2.59 ppm; (b) the protons of the methylenes naphthalene-CH₂-imidazolium and imidazolium-CH₂-anthracene appear as four different singlets around $\delta = 5.12$ and 5.50 ppm and $\delta = 6.18$ and 6.45 ppm, respectively; and (c) the protons of the naphthalene and the anthracene groups are embedded in the aromatic region in the range $\delta = 6.94$ –8.79 ppm.

The addition of increase amounts of H₂PO₄[−] (Figure 5) anions to a solution of the receptor 5²⁺·2PF₆[−] in CD₃CN/CD₃OD (8/2) induced the splitting and a significant downfield shifts of the inner naphthalene protons *H*_{*a,a'*} ($\Delta\delta \sim 0.23$ ppm). The methylene protons *H*_{*b*}, *H*_{*b'*}, *H*_{*c*} and *H*_{*c'*} were also downfield shifted; $\Delta\delta = 0.09$, 0.11, 0.05 and 0.07 ppm, respectively. Unfortunately the observation of the downfield shift of the H-imidazolium proton was not detected due to the signal of this proton within the aromatic region; nevertheless, the simultaneous participation in the anion binding process of the H and the Br sited at C-2 of the H-imidazolium and Br-imidazolium rings, respectively, was supported by the upfield shift observed in the methyl protons of the Br-imidazolium ring *H*_{*d*} ($\Delta\delta = -0.16$ ppm) and in the methyl protons *H*_{*e'*} of the H-imidazolium ring ($\Delta\delta = -0.10$ ppm) (Figure S13).

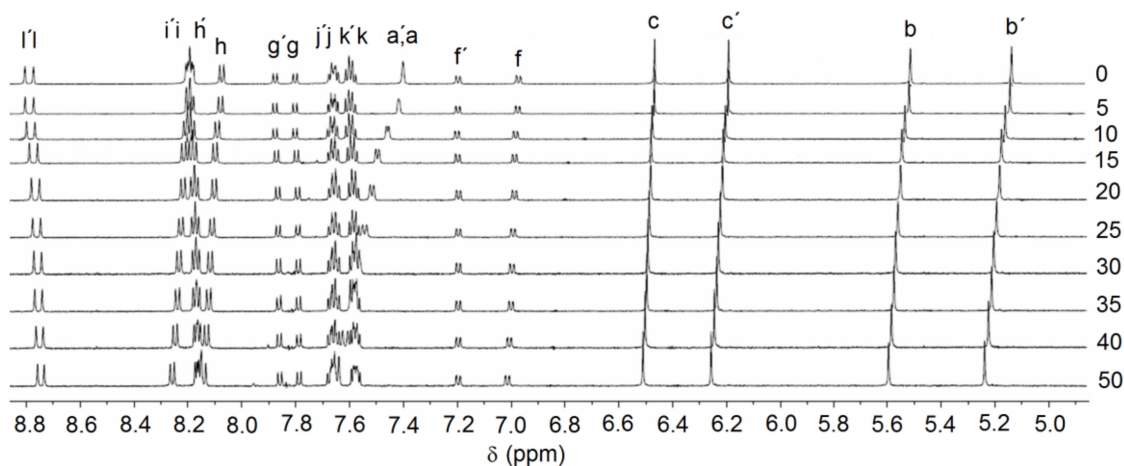
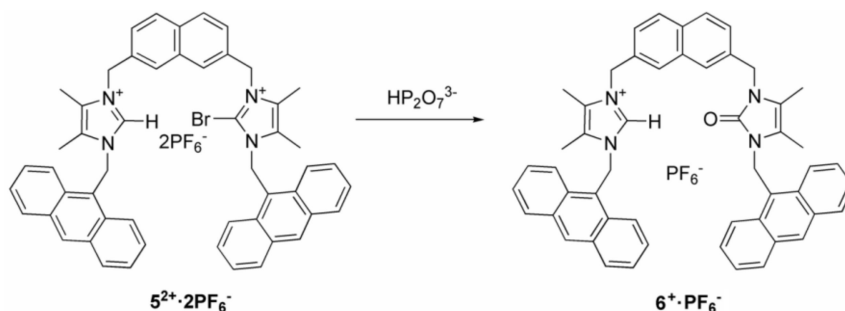


Figure 5. ¹H-NMR spectral changes observed in the receptor 5²⁺·2PF₆[−] in CD₃CN/CD₃OD (8/2, v/v) during the addition from 0 (top) to 50 equiv. (bottom) of H₂PO₄[−] anions.

Similar changes were observed with the presence of SO₄^{2−} anions but to a lesser extent than those produced with H₂PO₄[−] anions (Figure S10).

The addition of increasing amounts of HP₂O₇^{3−} (Figure S11) and F[−] anions (Figure S12) to a solution of the hydrogen and halogen bonding receptor 5²⁺·2PF₆[−] produce different changes in the ¹H-NMR than those previously described for H₂PO₄[−] and SO₄^{2−} anions. In these cases, the addition of HP₂O₇^{3−} and F[−] anions up to 1 equiv. promote the downfield shift of the internal naphthalene protons *H*_{*a,a'*} ($\Delta\delta \sim 0.09$ ppm) as well as the methylene protons *H*_{*b*}, *H*_{*b'*}, *H*_{*c*} and *H*_{*c'*} ($\Delta\delta \sim 0.03$ ppm), suggesting that a recognition processes is taking place. However, the addition of more than 1 equiv. of HP₂O₇^{3−} induced the appearance of new signals and the progressive disappearance of the signals assigned to the complexes formed between the receptor 5²⁺·2PF₆[−] with HP₂O₇^{3−} or F[−] anions. After addition of 2 equiv. of anion, the ¹H-NMR spectrum showed only one set of signals. The titration was also followed by mass spectrometry. The results indicate that a debromination process is taking place in the bromo-imidazolium ring by the formation of an imidazolone ring to generate the new compound 6²⁺·PF₆[−] (Scheme 2). Interestingly the H-imidazolium ring remains unperturbed in the presence of HP₂O₇^{3−} and F[−] anions. These results are consistent with those reported previously for the halogen and hydrogen bonding receptor 7²⁺·2PF₆[−] and 8²⁺·2PF₆[−], respectively [10] and dramatically reveal the lability of the C2–X bond of the haloimidazolium ring that undergoes cleavage in the presence of

basic anions, which constitutes a clear and important limitation for the use of such kind of receptors against basic anions.



Scheme 2. Synthesis of imidazolone $6^{2+} \cdot \text{PF}_6^{-}$ from the receptor $5^{2+} \cdot 2\text{PF}_6^{-}$ by the $\text{HP}_2\text{O}_7^{3-}$ anion.

The association constants calculated from the $^1\text{H-NMR}$ titration data using the Dynafit program [15] are shown in Table 2.

Table 2. Association constants for receptors $5^{2+} \cdot 2\text{PF}_6^{-}$, $7^{2+} \cdot 2\text{PF}_6^{-}$ and $8^{2+} \cdot 2\text{PF}_6^{-}$ with $\text{H}_2\text{PO}_4^{-}$ and SO_4^{2-} anions in $\text{CD}_3\text{CN}/\text{CD}_3\text{OD}$ 8:2 *v/v* measured using the $^1\text{H-NMR}$ technique. Errors (in percent) are given in parentheses.

Receptor	$\text{H}_2\text{PO}_4^{-}$	SO_4^{2-}	$K(\text{SO}_4^{2-})/\beta(\text{H}_2\text{PO}_4^{-})$
$5^{2+} \cdot \text{PF}_6^{-}$	$\beta = 1.37 \times 10^2 \text{ M}^{-2}$ (4)	$K = 2.6 \times 10^3 \text{ M}^{-1}$ (4)	18
$7^{2+} \cdot 2\text{PF}_6^{-}$	$\beta = 9.9 \times 10^3 \text{ M}^{-2}$ (3)	$K = 5.5 \times 10^3 \text{ M}^{-1}$ (4)	0.55
$8^{2+} \cdot 2\text{PF}_6^{-}$	$\beta = 5.6 \times 10^3 \text{ M}^{-2}$ (4)	$K = 2.2 \times 10^3 \text{ M}^{-1}$ (4)	0.39

A comparative study of the association constants obtained for the receptor $5^{2+} \cdot \text{PF}_6^{-}$ with those reported for the halogen bonding receptor $7^{2+} \cdot 2\text{PF}_6^{-}$ and the hydrogen bonding receptor $8^{2+} \cdot 2\text{PF}_6^{-}$ in the competitive mixture $\text{CD}_3\text{CN}/\text{CD}_3\text{OD}$ 8:2 *v/v* indicates that the receptors bind the SO_4^{2-} anions following the trend $7^{2+} \cdot 2\text{PF}_6^{-}$ (XB receptor) > $5^{2+} \cdot \text{PF}_6^{-}$ (XB and HB) > $8^{2+} \cdot 2\text{PF}_6^{-}$ (HB). Thus, the presence of halogen bonding interactions increases the strength of the receptors for SO_4^{2-} anion. Interestingly, the association constant between the receptor $5^{2+} \cdot \text{PF}_6^{-}$ and SO_4^{2-} anions is 18 times higher than with the $\text{H}_2\text{PO}_4^{-}$ anion, while higher association constants for the receptors $7^{2+} \cdot 2\text{PF}_6^{-}$ and $8^{2+} \cdot 2\text{PF}_6^{-}$ were found for $\text{H}_2\text{PO}_4^{-}$ anion, and therefore the halogen and hydrogen bonding receptor $5^{2+} \cdot \text{PF}_6^{-}$ is the receptor which shows the highest selectivity for SO_4^{2-} anions.

3. Experimental Section

3.1. General Comments

All reactions were carried out using solvents that were dried by routine procedures. All melting points were determined by means of a Kofler hot-plate melting-point apparatus (Wagner & Munz, München, Germany) and are uncorrected. Solution $^1\text{H-}$ and $^{13}\text{C-}$ spectra were recorded with Bruker 200, 300, 400, or 600 MHz spectrometers (Bruker Corporation, Billerica, MA, USA). The following abbreviations have been used to state the multiplicity of the signals: s (singlet), m (multiplet), and q (quaternary carbon atom). Chemical shifts (δ) in the $^1\text{H-}$ and $^{13}\text{C-NMR}$ spectra are referenced to tetramethylsilane (TMS). UV–vis and fluorescence spectra were carried out in the solvents and concentrations stated in the text and in the corresponding figure captions, using a dissolution cell with 10 mm path length, and they were recorded with the spectra background corrected before and after

sequential additions of different aliquots of anions. Quantum yield values were measured with respect to anthracene as the standard ($\Phi = 0.27 \pm 0.01$) using the equation:

$$\Phi_x/\Phi_s = (S_x/S_s)((1 - 10^{-As})/(1 - 10^{-Ax}))(n_s^2/n_x^2) \quad (1)$$

where x and s indicate the unknown and standard solution, respectively, Φ is the quantum yield, S is the area under the emission curve, A is the absorbance at the excitation wavelength and n is the refractive index. Mass spectra were recorded with a MLC-MS TOF 6220 (Agilent Technologies Germany, Waldbronn, Germany).

3.2. General Procedure for Synthesis of Compounds 2 and 4

To a solution of 4,5-dimethyl-1H-imidazol (0.27 g, 2.81 mmol) or 2-bromo-4,5-dimethyl-1H-imidazol (0.3 g, 1.71 mmol) in CH₃CN (120 mL) was added dropwise an aqueous solution of 1 M NaOH (3.27 mmol). The reaction medium was stirred for 10 min and after this time, 9-(bromomethyl)anthracene (0.5 g, 1.75 mmol) was added in one portion; the resulting mixture was stirred at 0 °C for 30 min in the case of compound 2 and 2h at room temperature for compound 4. The resulting precipitate was separated by filtration and purified by silica gel column chromatography (CH₂Cl₂/CH₃OH 95:5) to yield compound 2. In the case of compound 4, the resulting precipitate was filtered and dissolved in CH₂Cl₂ (50 mL) and then washed with water (2 × 50 mL). The organic solvent was collected and dried with anhydrous Na₂SO₄. After filtration, the solvent was removed under reduced pressure to yield the desired compound.

1-((anthracen-9-yl)methyl)-4,5-dimethyl-1H-imidazole (2). Yellow solid, yield 19%, ¹H-NMR (CDCl₃, 400 MHz) δ = 8.55 (s, 1H); 8.06–8.01 (m, 4H), 7.53–7.46 (m, 4H); 6.56 (s, 1H); 5.76 (s, 2H); 2.41 (s, 3H); 2.18 (s, 3H); ¹³C-NMR (CDCl₃, 100 MHz) δ = 134.3; 133.6; 131.4; 130.9; 129.3; 127.3; 125.3; 124.1; 123.1; 122.2; 41.7; 12.7; 9.0; MS (ESI, *m/z*): 287.10 [M + H]⁺.

1-((anthracen-9-yl)methyl)-2-bromo-4,5-dimethyl-1H-imidazole (4). Yield 48%, ¹H-NMR (CDCl₃, 400 MHz) δ = 8.48 (s, 1H); 8.10–8.05 (m, 4H), 7.57–7.48 (m, 4H); 6.06 (s, 2H); 1.97 (s, 3H); 1.22 (s, 3H); ¹³C-NMR (CDCl₃, 100 MHz) δ = 135.6; 132.1; 131.6; 130.4; 130.3; 128.1; 127.5; 126.1; 125.1; 124.1; 117.1; 45.4; 12.9; 10.9; MS (ESI, *m/z*): 364.08 [M + H]⁺.

3.3. Synthesis of Compound 3⁺·Br[−]

To a solution of compound 2 (0.25 g, 0.87 mmol) in CH₃CN (180 mL), 2,7-bis(bromomethyl)naphthalene (0.65 g, 2 mmol) was added in one portion. The mixture was stirred for 90 min at 60 °C; the volatile compounds were removed under vacuum and the resulting residue was purified by silica gel column chromatography (CH₂Cl₂/CH₃OH 9:1) to yield compound 3 as bromide salt. Yield 63%, ¹H-NMR (CDCl₃, 400 MHz) δ = 9.54 (s, 1H); 8.57 (s, 1H), 8.35 (d, 2H, *J* = 9 Hz), 8.06 (d, 2 H, *J* = 9 Hz), 7.73–7.66 (m, 5H); 7.40–7.46 (m, 4H), 6.45 (s, 2H); 5.48 (s, 2H); 4.71 (s, 1H), 4.61 (s, 1H), 2.03 (s, 3H); 1.66 (s, 3H); ¹³C-NMR (CDCl₃, 75 MHz) δ = 136.0; 135.4; 132.8; 132.5; 131.2; 131.0; 130.7; 130.6; 129.6; 128.9; 128.4; 128.2; 127.9; 127.6; 127.4; 126.4; 125.5; 125.0; 122.9; 121.3; 50.9; 45.1; 33.6; 9.7; 8.7; MS (ESI, *m/z*): 519.20 [M]⁺.

3.4. Synthesis of Receptor 5²⁺·2Br[−]

To a solution of compound 3⁺·Br[−] (0.3 g, 0.5 mmol) in acetonitrile (200 mL), compound 4 (0.36 g, 0.98 mmol) was added. The reaction mixture was stirred at 60 °C for 48 h. The solvent was then removed under reduced pressure and the crude was purified by silica gel column chromatography (CH₂Cl₂/CH₃OH 9:1) to yield the desired compound as bromide salt. Yield 25%, ¹H-NMR (*d*₆-DMSO, 300 MHz) δ = 8.90 (s, 1H); 8.83 (s, 1H), 8.38 (d, 2H, *J* = 9 Hz), 8.30 (s, 1H), 8.26–8.17 (m, 6H), 7.95 (d, 1H, *J* = 9 Hz), 7.88 (d, 1H, *J* = 8 Hz), 7.70–7.55 (m, 10H), 7.23 (dd, 1H, *J* = 9 Hz, *J* = 0.5 Hz), 7.00 (dd, 1H, *J* = 9 Hz, *J* = 0.5 Hz), 6.62 (s, 2H), 6.37 (s, 2H), 5.66 (s, 2H), 5.34 (s, 2H); 2.59 (s, 3H), 2.17 (s, 3H); 2.13 (s, 3H), 1.82 (s, 3H); ¹³C-NMR (*d*₆-DMSO, 75 MHz) δ = 135.6; 134.4; 133.8; 133.3; 132.6; 132.3; 132.1;

131.8; 131.5; 131.3; 131.1; 130.9; 130.2; 130.1; 129.1; 129.0; 128.3; 127.2; 127.1; 126.9; 126.4; 126.2; 125.8; 125.0; 124.7; 124.3; 123.4; 122.9; 51.6; 50.8; 48.5; 45.1; 11.4; 10.4; 9.5; MS (ESI, m/z): 885.2 [$M^{2+} + Br^{-}$] $^{+}$.

3.5. Synthesis of Receptor $5^{2+} \cdot 2PF_6^{-}$

A solution of the bis-imidazolium receptor as the bromide salt $5^{2+} \cdot 2Br^{-}$ (0.1 g, 0.1 mmol) in CH_2Cl_2 (20 mL) was washed with a saturated solution of NH_4PF_6 (4×20 mL) for 30 min. The organic layer was separated, dried over anhydrous Na_2SO_4 , filtered and evaporated under reduced pressure, yielding the desired receptor. Yield 62%, 1H -NMR (d_6 -DMSO, 400 MHz) δ = 8.90 (s, 1H); 8.83 (s, 1H), 8.33 (d, 2H, J = 8 Hz), 8.30 (s, 1H), 8.26 (d, 2H, J = 8 Hz), 8.22 (d, 2H, J = 8 Hz), 8.14 (d, 2H, J = 8 Hz), 7.94 (d, 1H, J = 8 Hz), 7.87 (d, 1H, J = 8 Hz), 7.70-7.58 (m, 8H), 7.53 (s, 1H), 7.49 (s, 1H), 7.19 (dd, 1H, J = 8 Hz, J = 0.5 Hz), 6.95 (dd, 1H, J = 8 Hz, J = 0.5 Hz), 6.57 (s, 2H), 6.33 (s, 2H), 5.65 (s, 2H), 5.32 (s, 2H); 2.58 (s, 3H), 2.17 (s, 3H); 2.13 (s, 3H), 1.40 (s, 3H); ^{13}C -NMR (d_6 -DMSO, 100 MHz) δ = 134.0; 132.9; 132.3; 132.0; 131.9; 131.2; 130.9; 130.8; 130.6; 130.4; 130.1; 129.7; 129.5; 128.9; 128.7; 128.6; 126.9; 125.9; 125.6; 125.5; 125.0; 124.8; 124.4; 123.4; 123.1; 122.8; 121.8; 121.3; 50.2; 48.4; 46.8; 43.5; 9.8; 8.9; 8.4; 7.9; MS (ESI, m/z): 951.2 [$M^{2+} + PF_6^{-}$] $^{+}$.

4. Conclusions

We have reported the synthesis of a novel anion sensor $5^{2+} \cdot 2PF_6^{-}$ which binds anions by the cooperative action of halogen- and hydrogen-bonding interactions. Several anion-binding experiments have been carried out in order to make a comparative study of the sensing capabilities of the novel XB and HB receptor $5^{2+} \cdot 2PF_6^{-}$ regarding the XB and HB analogues $7^{2+} \cdot 2PF_6^{-}$ and $8^{2+} \cdot 2PF_6^{-}$, respectively. Evaluation of the sensing properties by fluorescence in CH_3CN reveals important similarities in the sensing behaviour between the halogenated receptor $7^{2+} \cdot 2PF_6^{-}$ and the mixed XB and HB receptor $5^{2+} \cdot 2PF_6^{-}$. The XB and HB receptor $5^{2+} \cdot 2PF_6^{-}$ acts as a selective fluorescent molecular sensor for $H_2PO_4^{-}$ anion, because it is the unique anion which promotes the appearance of the anthracene excimer emission band. In addition, the presence of the $HP_2O_7^{3-}$ anion produces the selective transformation in the corresponding mono-imidazolone $6^{2+} \cdot 2PF_6^{-}$ after debromination of the Br-imidazolium ring while the H-imidazolium ring remained unperturbed. The analysis of the obtained association constant values obtained from the 1H -NMR titration experiments in $CD_3CN/MeOD$ (8/2) reveals that the selectivity showed for the mixed XB and HB receptor $5^{2+} \cdot 2PF_6^{-}$ for SO_4^{2-} anions is higher than the ones observed for the halogen or hydrogen bonding analogues. The magnitude of the association constant with SO_4^{2-} anions of the mixed XB and HB receptor $5^{2+} \cdot 2PF_6^{-}$ is intermediate between the halogen bonding receptor $7^{2+} \cdot 2PF_6^{-}$ and the hydrogen bonding receptor $8^{2+} \cdot 2PF_6^{-}$ in this competitive methanolic medium. These results highlight the importance of the combinations of different non-covalent interactions in selective anion recognition and sensing.

Supplementary Materials: The supplementary materials are available online. 1H - and ^{13}C -NMR spectra of the compound, Figures S1–S3: Changes in the emission spectrum of $5^{2+} \cdot 2PF_6^{-}$ upon addition of F^{-} and AcO^{-} anions, Figures S4–S6: Calculation of the detection limits, Figures S7–S9: Job's Plot experiments, Figures S10–S13: 1H -NMR spectral changes of the receptor $5^{2+} \cdot 2PF_6^{-}$ during the addition of SO_4^{2-} , $HP_2O_7^{3-}$ and F^{-} anions.

Acknowledgments: This work was funded by the Ministerio de Economía y Competitividad Government of Spain and European FEDER CTQ2013-46096-P as well as by the Fundación Séneca Región de Murcia (CARM) Projects 18948/JLI/13 and 19337/PI/14. P.S. acknowledges the University of Murcia for a FPU predoctoral grant. F.Z. and A.C. acknowledge the Government of Spain for a Juan de la Cierva and Ramon y Cajal contract, respectively.

Author Contributions: F.Z., A.C. and P.M. conceived and designed the experiments; F.Z., P.S. and S.J.B.-B. performed the experiments; F.Z., P.S., S.B., A.C. and P.M. analyzed the data; F.Z., A.C. and P.M. wrote the paper.

Conflicts of Interest: The authors declare no conflict of interest.

References

1. Evans, N.H.; Beer, P.D. Advances in anion supramolecular chemistry: From recognition to chemical applications. *Angew. Chem. Int. Ed.* **2014**, *53*, 11716–11754. [[CrossRef](#)] [[PubMed](#)]

2. Gale, P.A.; Busschaert, N.; Haynes, C.J.E.; Karagiannidis, L.E.; Kirby, I.L. Anion receptor chemistry: Highlights from 2011 and 2012. *Chem. Soc. Rev.* **2014**, *43*, 205–241. [[CrossRef](#)] [[PubMed](#)]
3. Santos-Figueroa, L.E.; Moragues, M.E.; Climent, E.; Agostini, A.; Martinez-Mañez, R.; Sancenon, F. Chromogenic and fluorogenic chemosensors and reagents for anions: A comprehensive review of the years 2010–2011. *Chem. Soc. Rev.* **2013**, *42*, 3489–3613. [[CrossRef](#)] [[PubMed](#)]
4. Gale, P.A.; Howe, E.N.W.; Wu, X. Anion receptor chemistry. *Chem. Commun.* **2016**, *1*, 351–422. [[CrossRef](#)]
5. Bondy, C.R.; Loeb, S.J. Amide Based Receptors for Anions. *Coord. Chem. Rev.* **2003**, *240*, 77–99. [[CrossRef](#)]
6. Amendola, V.; Fabbrizzi, L.; Mosca, L. Anion recognition by hydrogen bonding: Urea-based receptors. *Chem. Soc. Rev.* **2010**, *39*, 3889–3915. [[CrossRef](#)] [[PubMed](#)]
7. Sessler, J.L.; Camiolo, S.; Gale, P.A. Pyrrolic and polypyrrolic anion binding agents. *Coord. Chem. Rev.* **2003**, *240*, 17–55. [[CrossRef](#)]
8. Molina, P.; Tarraga, A.; Oton, F. Imidazole derivatives: A comprehensive survey of their recognition properties. *Org. Biomol. Chem.* **2012**, *10*, 1711–1724. [[CrossRef](#)] [[PubMed](#)]
9. Scheiner, S. Halogen bonds formed between substituted imidazolium and N bases of varying N-hybridization. *Molecules* **2017**, *22*, 1634. [[CrossRef](#)] [[PubMed](#)]
10. Metrangolo, P.; Meyer, F.; Pilati, T.; Resnati, G.; Terraneo, G. Halogen bonding in supramolecular chemistry. *Angew. Chem. Int. Ed.* **2008**, *47*, 6114–6127. [[CrossRef](#)] [[PubMed](#)]
11. Politzer, P.; Murray, J.S.; Clark, T. Halogen bonding: An electrostatically-driven highly directional noncovalent interaction. *Phys. Chem. Chem. Phys.* **2010**, *12*, 7748–7757. [[CrossRef](#)] [[PubMed](#)]
12. Molina, P.; Zapata, F.; Caballero, A. Anion recognition strategies based on combined noncovalent interactions. *Chem. Rev.* **2017**, *117*, 9907–9972. [[CrossRef](#)] [[PubMed](#)]
13. Chmielewski, M.J.; Davis, J.J.; Beer, P.D. Interlocked host rotaxane and catenane structures for sensing charged guest species via optical and electrochemical methodologies. *Org. Biomol. Chem.* **2009**, *7*, 415–429. [[CrossRef](#)] [[PubMed](#)]
14. Lankshear, M.D.; Beer, P.D. Interweaving anion templation. *Acc. Chem. Res.* **2007**, *40*, 657–668. [[CrossRef](#)] [[PubMed](#)]
15. Kilah, N.L.; Wise, M.D.; Serpell, C.J.; Thompson, A.L.; White, N.G.; Christensen, K.E.; Beer, P.D. Enhancement of anion recognition exhibited by a halogen-bonding rotaxane host system. *J. Am. Chem. Soc.* **2010**, *132*, 11893–11895. [[CrossRef](#)] [[PubMed](#)]
16. Mullaney, B.R.; Partridge, B.E.; Beer, P.D. A halogen-bonding bis-triazolium rotaxane for halide-selective anion recognition. *Chemistry* **2015**, *21*, 1660–1665. [[CrossRef](#)] [[PubMed](#)]
17. Langton, M.J.; Robinson, S.W.; Marques, I.; Félix, V.; Beer, P.D. Halogen bonding in water results in enhanced anion recognition in acyclic and rotaxane hosts. *Nat. Chem.* **2014**, *6*, 1039–1043. [[CrossRef](#)] [[PubMed](#)]
18. Langton, M.J.; Marques, I.; Robinson, S.W.; Félix, V.; Beer, P.D. Iodide recognition and sensing in water by a halogen-bonding ruthenium(II)-based rotaxane. *Chemistry* **2016**, *22*, 185–192. [[CrossRef](#)] [[PubMed](#)]
19. Caballero, A.; Swan, L.; Zapata, F.; Beer, P.D. Iodide-induced shuttling of a halogen- and hydrogen-bonding two-station rotaxane. *Angew. Chem. Int. Ed.* **2014**, *53*, 11854–11858. [[CrossRef](#)] [[PubMed](#)]
20. Gilday, L.C.; Beer, P.D. Halogen- and hydrogen-bonding catenanes for halide-anion recognition. *Chemistry* **2014**, *20*, 8379–8385. [[CrossRef](#)] [[PubMed](#)]
21. Mercurio, J.M.; Caballero, A.; Cookson, J.; Beer, P.D. A halogen- and hydrogen-bonding [2]catenane for anion recognition and sensing. *RSC Adv.* **2015**, *5*, 9298–9306. [[CrossRef](#)]
22. Robinson, S.W.; Mustoe, C.L.; White, N.G.; Brown, A.; Thompson, A.L.; Kennepohl, P.; Beer, P.D. Evidence for halogen bond covalency in acyclic and interlocked halogen-bonding receptor anion recognition. *J. Am. Chem. Soc.* **2015**, *137*, 499–507. [[CrossRef](#)] [[PubMed](#)]
23. Chudzinski, M.G.; McClary, C.A.; Taylor, M.S. Anion receptors composed of hydrogen- and halogen-bond donor groups: Modulating selectivity with combinations of distinct noncovalent interactions. *J. Am. Chem. Soc.* **2011**, *133*, 10559–10567. [[CrossRef](#)] [[PubMed](#)]
24. Sabater, P.; Zapata, F.; Caballero, A.; Visitación, N.; Alkorta, I.; Elguero, J.; Molina, P. Comparative study of charge-assisted hydrogen- and halogen-bonding capabilities in solution of two-armed imidazolium receptors toward oxoanions. *J. Org. Chem.* **2016**, *81*, 7448–7458. [[CrossRef](#)] [[PubMed](#)]
25. D'Sa, A.; Cohen, L.A.J. 4,5-Dimethylimidazole: A correction and alternative synthesis. *Heterocycl. Chem.* **1991**, *28*, 1819–1820. [[CrossRef](#)]

26. Serpell, C.J.; Kilah, N.L.; Costa, P.J.; Felix, V.; Beer, P.D. Halogen bond anion templated assembly of an imidazolium pseudorotaxane. *Angew. Chem. Int. Ed.* **2010**, *49*, 5322–5326. [[CrossRef](#)] [[PubMed](#)]
27. Gunnlaugsson, T.; Glynn, M.; Tocci, G.M.; Kruger, P.E.; Pfeffer, F.M. Anion recognition and sensing in organic and aqueous media using luminescent and colorimetric sensors. *Coord. Chem. Rev.* **2006**, *250*, 3094–3117. [[CrossRef](#)]
28. De Silva, P.; Gunaratne, H.Q.N.; Gunnlaugsson, T.; Huxley, A.J.M.; McCoy, C.P.; Rademacher, J.T.; Rice, T.E. Signaling recognition events with fluorescent sensors and switches. *Chem. Rev.* **1997**, *97*, 1515–1566. [[CrossRef](#)] [[PubMed](#)]
29. Kuzmic, P. Program DYNAFIT for the analysis of enzyme kinetic data: application to HIV proteinase. *Anal. Biochem.* **1996**, *237*, 260–273. [[CrossRef](#)] [[PubMed](#)]

Sample Availability: Samples of the compounds are not available from the authors.



© 2017 by the authors. Licensee MDPI, Basel, Switzerland. This article is an open access article distributed under the terms and conditions of the Creative Commons Attribution (CC BY) license (<http://creativecommons.org/licenses/by/4.0/>).